Analytic gradients for excited states in the coupled-cluster model CC2 employing the resolution-of-the-identity approximation

Andreas Köhn[a)]
Universität Karlsruhe (TH), Institut für Physikalische Chemie, Lehrstuhl für Theoretische Chemie, Kaiserstraße 12, D-76128 Karlsruhe, Germany

Christof Hättig
Forschungszentrum Karlsruhe, Institute of Nanotechnology, P.O. Box 3640, D-76021 Karlsruhe, Germany

(Received 13 May 2003; accepted 11 June 2003)

The derivation and implementation of excited state gradients is reported for the approximate coupled-cluster singles and doubles model CC2 employing the resolution-of-the-identity approximation for electron repulsion integrals. The implementation is profiled for a set of examples with up to 1348 basis functions and exhibits no I/O bottlenecks. A test set of sample molecules is used to assess the performance of the CC2 model for adiabatic excitation energies, excited state structure constants and vibrational frequencies. We find very promising results, especially for adiabatic excitation energies, though the need of a single-reference ground state and a single-replacement dominated excited state puts some limits on the applicability of the method. Its reliability, however, can always be tested on grounds of diagnostic measures. As an example application, we present calculations on the $\pi^* \leftarrow \pi$ excited state of *trans*-azobenzene. © *2003 American Institute of Physics.* [DOI: 10.1063/1.1597635]

I. INTRODUCTION

The Born–Oppenheimer approximation is probably the most fundamental concept of quantum chemistry. It defines a set of potential-energy hypersurfaces which are functions of the nuclear configuration space each of which can be associated with different electronic states of the molecules. Stationary points on these surfaces are of particular interest as they define equilibrium and transition structures. Locating these stationary points is one of the basic tasks in computational chemistry. A number of efficient algorithms have been developed for this purpose, for which—apart from the energy—the knowledge of the analytical gradient is an important ingredient. Starting with the pioneering work of Pulay[1,2] gradient methods for ground states have become standard tools in modern quantum chemistry.

For excited states, however, gradient codes are still far from being a standard tool in applications, though an increasing number of implementations for various methods is available.[3–13] The vast majority of studies dealing with excited states are confined to vertical excitation energies, i.e., the electronic energy difference between ground and excited state at the ground state equilibrium structure. By virtue of the Franck–Condon principle, the most intense vibronic transition (or the band maximum in case of low-resolution spectra) often is identified with a vertical transition, but strictly speaking, vertical excitation energies are not well defined physical observables. It has been shown in calculations that include vibronic coupling, that the deviation of band maximum and vertical transition can be on the order of more than 0.1 eV.[14,15] Above that, for a highly resolved spectrum, more detailed information is desired, such as the position of the 0–0 transition (i.e., the transition between the two lowest vibrational levels of the two electronic states), the effects on the molecular structure and the assignment of vibrational progressions. Similarly, for the investigation of fluorescence spectra the knowledge of the relaxed excited state structure is inevitable.

In this paper we report an implementation of excited state analytic gradients for the approximate coupled-cluster singles and doubles model CC2[16] employing the resolution-of-the-identity (RI) approximation[17–19] for two-electron repulsion integrals. Coupled-cluster theory[20] has in recent time become very popular, as it offers a hierarchy of size-consistent wave-function models with increasing accuracy.[21] Excited states are accessible by applying response theory to the underlying coupled-cluster wave-function model.[22–25] With respect to excited state gradient theory, pioneering work has been carried out by Stanton and Gauss for the coupled-cluster singles and doubles model CCSD.[7,26,27] This code has later been modified[28] to obtain an experimental version of analytical gradients for the approximate coupled-cluster singles and doubles model CC2. The computational effort of that method scales with the fifth power of the molecular size, unlike for other approximations to CCSD, like EOM–CCSD(2)[29] and P–EOM–MBPT(2),[9] where some steps with a higher scaling remain [CIS(D),[8,30] on the other hand, can be viewed as a noniterative approximation to CC2; we will shortly comment on this issue in Sec. IV C]. Results from applications of CC2 to benzene[28] and pyrrol[31] were found to be rather encouraging, as CC2 clearly improves on CIS[5] (configuration interaction in the space of—relative to a Hartree–Fock state—singly excited determinants). Applying

[a)]Current address: Forschungszentrum Karlsruhe, Institute of Nanotechnology, P.O. Box 3640, D-76021 Karlsruhe, Germany; Electronic mail: andreas.koehn@chemie.uni-karlsruhe.de

 © 2003 American Institute of Physics

Downloaded 13 Feb 2004 to 141.52.232.84. Redistribution subject to AIP license or copyright, see http://jcp.aip.org/jcp/copyright.jsp

the RI approximation to CC2 (RI–CC2) facilitates the implementation of a T_2-direct code,[32–34] which avoids the I/O bottleneck due to four-index intermediates. It thereby extends the applicability of CC2 to comparatively large systems with more than 1000 basis functions.

In the following sections, we describe the derivation and implementation of analytic gradients of RI–CC2 excited state energies (Secs. II and III). In Sec. IV, the accuracy of the RI approximation is tested for adiabatic excitation energies and excited state structures and the applicability of the approach to large systems is demonstrated. Thereafter, the performance of the CC2 model is assessed for a set of 20 sample molecules. As an example for a typical application, the $\pi^* \leftarrow \pi$ excited state of *trans*-azobenzene is discussed in Sec. V.

II. EXCITED STATE GRADIENT THEORY FOR CC2

A. The relaxed excited state Lagrange function

The derivation of the excited state gradient parallels in many respects the one for the ground state case in Ref. 34. Similar as for the ground state, we define a Lagrange function for the total energy of an excited state f:

$$L^f = \langle \mathrm{HF}|\hat{H}+[\hat{H},T_2]|\mathrm{HF}\rangle + \sum_{i,j=1}^{2} \sum_{\mu_i \nu_j} \overline{E}^f_{\mu_i} A_{\mu_i \nu_j} E^f_{\nu_j} + \overline{\omega}^f \left(1 - \sum_{i=1}^{2} \sum_{\mu_i} \overline{E}^f_{\mu_i} E^f_{\mu_i} \right) + \sum_{i=1}^{2} \sum_{\mu_i} \overline{t}^f_{\mu_i} \Omega_{\mu_i} + \sum_{\mu_0} \overline{\kappa}^f_{\mu_0} F_{\mu_0}. \quad (1)$$

This form of the Lagrange function for the total energy of an excited state in coupled-cluster response theory was suggested by Christiansen *et al.*[35] (cf. also Ref. 36). An alternative formulation within the equation-of-motion formalism was given by Stanton.[26] The first term of Eq. (1) gives the coupled-cluster ground state energy, where $|\mathrm{HF}\rangle$ is the Hartree–Fock reference state and $T_i = \Sigma_{\mu_i} t_{\mu_i} \tau_{\mu_i}$ are the cluster operators consisting of the cluster amplitudes t_{μ_i} and the singlet adapted excitation operators τ_{μ_i}.[80] With μ_1 we denote single replacements, e.g., $\tau_{\mu_1} = \tau_{ai}$ and likewise μ_2 is a shortcut for double replacements; furthermore the usual convention for occupied $(i,j,k,\ldots)$, virtual $(a,b,c,\ldots)$ and general indices $(p,q,r,\ldots)$ is adopted. It is convenient to introduce the T_1-transformed Hamiltonian[37]

$$\hat{H} = e^{-T_1} H e^{T_1} = \sum_{pq} \hat{h}_{pq} \tau_{pq} + \tfrac{1}{2} \sum_{pqrs} (pq\hat{|}rs) \tau^{(-)}_{pqrs}, \quad (2)$$

where the integrals $\hat{h}_{pq}$ and $(pq\hat{|}rs)$ are related to the respective quantities in the canonical molecular orbital (MO) basis by the transformation matrices $\lambda^p = (\mathbf{1} - \mathbf{t}_1^T)$ and $\lambda^h = (\mathbf{1} + \mathbf{t}_1)$, e.g., $\hat{h}_{rs} = \Sigma_{r's'} \lambda^p_{r'r} \lambda^h_{s's} h_{r's'}$. Contracting these transformation matrices with the usual MO coefficient matrix $\mathbf{C}$ yields $\Lambda^p = \mathbf{C}\lambda^p$ and $\Lambda^h = \mathbf{C}\lambda^h$. We will refer to this basis as Λ^p, Λ^h-basis.[37]

The last two terms of the Lagrangian in Eq. (1) are also present in the ground state expression. The first one, containing the Lagrange multiplier $\overline{t}$, ensures that the CC2 ground state equations

$$\Omega_{\mu_1} = \langle \mu_1 | \hat{H} + [\hat{H}, T_2] | \mathrm{HF} \rangle = 0, \quad (3)$$

$$\Omega_{\mu_2} = \langle \mu_2 | \hat{H} + [F, T_2] | \mathrm{HF} \rangle = 0 \quad (4)$$

are fulfilled, where F is the usual Fock operator.

The other term, containing the Lagrange multiplier $\overline{\kappa}$, implements the constraint that the subspace μ_0 of the Fock matrix elements is zero, where one can either require a diagonal Fock matrix (canonical condition) or that only the Brillouin condition be fulfilled ($F_{ia} = 0$). The Hartree–Fock state is parametrized as

$$|\mathrm{HF}\rangle = \sum_{\mu_0} \exp(\kappa_{\mu_0}(\tau_{\mu_0} - \tau^\dagger_{\mu_0}))|\mathrm{HF}_0\rangle, \quad (5)$$

where $|\mathrm{HF}_0\rangle$ is the unperturbed state. If the perturbation is a geometrical distortion some more care is appropriate: $|\mathrm{HF}_0\rangle$ then is a state in the orthonormalized MO (OMO) basis at the new nuclear coordinates, generated from the MOs at the unperturbed geometry by a connection matrix.[38] This will give rise to an additional term in the gradient expression involving the derivative of the overlap matrix (*vide infra*).

The second term in Eq. (1) occurs only in the excited state Lagrangian: It yields the excitation energy $\overline{E}^f \mathbf{A} E^f = \omega^f$, i.e., in combination the first two terms sum up to the total energy of the molecular system in an excited state. $\overline{E}$ and E are the left and right eigenvectors of the nonsymmetric Jacobian

$$A_{\mu\nu} = \frac{\partial \Omega_\mu}{\partial t_\nu}. \quad (6)$$

The subsequent term in the Lagrange function ensures the biorthonormality of $\overline{E}$ and E. The derivative of the Lagrangian with respect to $\overline{E}$ (E) leads to the right (left) eigenvalue problem of $\mathbf{A}$ and reveals that $\overline{\omega}^f = \omega^f$.

B. Excited state relaxed one- and two-particle densities

The CC2 model can be implemented very efficiently using the resolution-of-the-identity (RI) approximation which allows for a fast AO to MO transformation

$$B^Q_{ai} = \sum_P \left(\sum_\alpha C_{\alpha a} \sum_\beta C_{\beta i} (\alpha\beta|P) \right) V^{-1/2}_{PQ} \quad (7)$$

and a subsequent fast formation of four-index integrals in the MO basis

$$(ai|bj) \approx (ai|bj)^{\mathrm{RI}} = \sum_Q B^Q_{ai} B^Q_{bj}. \quad (8)$$

In the latter equations $V_{PQ} = (P|Q)$ and $(\alpha\beta|P)$ are, respectively, two- and three-index electron repulsion integrals. Since only N^3-scaling intermediates are needed on disk, the I/O requirements are reduced drastically compared to a conventional four-index transformation. For further details about

Downloaded 13 Feb 2004 to 141.52.232.84. Redistribution subject to AIP license or copyright, see http://jcp.aip.org/jcp/copyright.jsp

the RI approximation, e.g., the choice of auxiliary basis sets and the accuracy obtained the reader is referred to Refs. 33 and 39.

In the present implementation the Hartree–Fock equations are still solved using conventional four-index integrals. Therefore, we need to distinguish carefully between contributions to the Lagrangian which arise from the reference state and the Fock operator and those which are calculated using the RI approximation. For this purpose, we rewrite the Lagrange function, Eq. (1), as

$$L=\langle \mathrm{HF}|H|\mathrm{HF}\rangle+\overline{\omega}(1-\overline{E}_{\mu}E_{\mu})+\sum_{pq}(D_{pq}^{F,\xi}(\overline{t})+D_{pq}^{F,A}(\overline{E},E))F_{pq}+\sum_{\mu_0}\overline{\kappa}_{\mu_0}F_{\mu_0}+\tfrac{1}{2}\sum_{pqrs}(\hat{d}_{pqrs}^{\mathrm{nsep},\xi}(\overline{t})+\hat{d}_{pqrs}^{\mathrm{nsep},A}(\overline{E},E))(pq\hat{|}rs)^{\mathrm{RI}}, \tag{9}$$

where the superscripts f are omitted for brevity. Here, we have introduced the one-particle densities

$$D_{pq}^{F,\xi}(\overline{t})=\langle \mathrm{HF}|[\tau_{pq},T_1]|\mathrm{HF}\rangle+\sum_{\mu_1}\overline{t}_{\mu_1}\langle\mu_1|e^{-T_1}\tau_{pq}e^{T_1}+[\tau_{pq},T_2]|\mathrm{HF}\rangle+\sum_{\mu_2}\overline{t}_{\mu_2}\langle\mu_2|[\tau_{pq},T_2]|\mathrm{HF}\rangle \tag{10}$$

and

$$D_{pq}^{F,A}(\overline{E},E)=\sum_{\mu_1\nu_1}\overline{E}_{\mu_1}\langle\mu_1|[\tau_{pq},\tau_{\nu_1}]+[[\tau_{pq},\tau_{\nu_1}],T_1]|\mathrm{HF}\rangle E_{\nu_1}+\sum_{\mu_1\nu_2}\overline{E}_{\mu_1}\langle\mu_1|[\tau_{pq},\tau_{\nu_2}]|\mathrm{HF}\rangle E_{\nu_2}+\sum_{\mu_2\nu_2}\overline{E}_{\mu_2}\langle\mu_2|[\tau_{pq},\tau_{\nu_2}]|\mathrm{HF}\rangle E_{\nu_2}. \tag{11}$$

These densities contain only contributions from the correlation treatment. The two-electron densities are most conveniently expressed in the Λ^p, Λ^h-basis, which is indicated by the notation $\hat{d}_{pqrs}$. They are connected to the densities in the MO basis by the contravariant transformation:

$$d_{pqrs}=\sum_{p'q'r's'}\lambda_{pp'}^{p}\lambda_{qq'}^{h}\lambda_{rr'}^{p}\lambda_{ss'}^{h}\hat{d}_{p'q'r's'}. \tag{12}$$

The two contributions to the nonseparable two-electron density read

$$\hat{d}_{pqrs}^{\mathrm{nsep},\xi}(\overline{t})=\langle \mathrm{HF}|[[\tau_{pqrs}^{(-)},T_1],T_1]+[\tau_{pqrs}^{(-)},T_2]|\mathrm{HF}\rangle+\sum_{\mu_1}\overline{t}_{\mu_1}\langle\mu_1|[\tau_{pqrs}^{(-)},T_1]+[\tau_{pqrs}^{(-)},T_2]|\mathrm{HF}\rangle+\sum_{\mu_2}\overline{t}_{\mu_2}\langle\mu_2|\tau_{pqrs}^{(-)}|\mathrm{HF}\rangle \tag{13}$$

and

$$\hat{d}_{pqrs}^{\mathrm{nsep},A}(\overline{E},E)=\sum_{\mu_1\nu_1}\overline{E}_{\mu_1}\langle\mu_1|[\tau_{pqrs}^{(-)},\tau_{\nu_1}]+[[\tau_{pqrs}^{(-)},\tau_{\nu_1}],T_2]|\mathrm{HF}\rangle E_{\nu_1}+\sum_{\mu_1\nu_2}\overline{E}_{\mu_1}\langle\mu_1|[\tau_{pqrs}^{(-)},\tau_{\nu_2}]|\mathrm{HF}\rangle E_{\nu_2}+\sum_{\mu_2\nu_1}\overline{E}_{\mu_2}\langle\mu_2|[\tau_{pqrs}^{(-)},\tau_{\nu_1}]|\mathrm{HF}\rangle E_{\nu_1}. \tag{14}$$

Explicit expressions for the densities are given in the supplement.[40] Note that only active orbitals contribute, i.e., the elements of D^F and d^{nsep} are nonzero only if all indices refer to active orbitals. The respective ground state densities (cf. Ref. 34) are recovered as $D_{pq}^{F}=D_{pq}^{F,\xi}(\overline{t}^{(0)})$ and $\hat{d}_{pqrs}^{\mathrm{nsep}}=\hat{d}_{pqrs}^{\mathrm{nsep},\xi}(\overline{t}^{(0)})$ where $\overline{t}^{(0)}$ are the ground state Lagrangian multipliers. $D^{F,A}$ and $\hat{d}^{\mathrm{nsep},A}$ contain the contributions from the eigenvectors, which do not have counterparts in the expressions for the ground state densities.

The implementation of the cluster equations and the solution of the eigenvalue and response equations for the amplitudes t, $\overline{t}$, E, and $\overline{E}$ in the RI–CC2 approach is described in Refs. 32 and 33. Note that the multipliers $\overline{t}$ used in the above equations correspond to the sum of the ground state multipliers $\overline{t}^{(0)}$ and the multipliers for the excitation energy $\overline{N}$ defined in Ref. 33. Thus, the response equation for $\overline{t}$ reads

$$\sum_{\mu}\overline{t}_{\mu}A_{\mu\nu}=\eta_{\nu}^{(0)}+\sum_{\mu\gamma}\overline{E}_{\mu}B_{\mu\gamma\nu}E_{\gamma}, \tag{15}$$

where the two right-hand side contributions contain the quantities

$$\eta_{\nu}^{(0)}=\frac{\partial\langle \mathrm{HF}|\hat{H}+[\hat{H},T_2]|\mathrm{HF}\rangle}{\partial t_{\nu}}\quad\text{and}\quad B_{\mu\gamma\nu}=\frac{\partial A_{\mu\gamma}}{\partial t_{\nu}}. \tag{16}$$

Explicit expressions for these terms are given in Refs. 33 and 34 and we refer the reader to these publications for details of the partitioned, doubles-direct formulation and implementation of the coupled-cluster response equations.

The orbital rotation Lagrangian multipliers $\overline{\kappa}$ are determined from a set of CPHF equations (also known as Z-vector equations)[41]

$$\sum_{AI}\overline{\kappa}_{AI}(A_{AIBJ}^{\kappa}-\delta_{AB}\epsilon_A-\delta_{IJ}\epsilon_I)=-\eta_{BJ}^{\kappa,f}. \tag{17}$$

Here, we introduced the convention that capital indices refer to both active and frozen orbitals. Orbital energies are denoted by ϵ_p and the matrix A^{κ} is defined as

$$A_{pqrs}^{\kappa}=4(pq|rs)-(pr|qs)-(ps|rq). \tag{18}$$

The right-hand side can be calculated from the one- and two-particle densities Eqs. (10)–(14):

Downloaded 13 Feb 2004 to 141.52.232.84. Redistribution subject to AIP license or copyright, see http://jcp.aip.org/jcp/copyright.jsp

$$\eta_{AI}^{\kappa,f}=\tfrac{1}{2}(D_{AI}^{F,\mathrm{ex}}+D_{IA}^{F,\mathrm{ex}})(\epsilon_I-\epsilon_A)-\tfrac{1}{4}\sum_{pq}(D_{pq}^{F,\mathrm{ex}}+D_{qp}^{F,\mathrm{ex}})A_{pqAI}$$
$$+\sum_{prs}[(d_{pArs}^{\mathrm{nsep,ex}}+d_{Aprs}^{\mathrm{nsep,ex}})(pI|rs)^{\mathrm{RI}}$$
$$-(d_{pIrs}^{\mathrm{nsep,ex}}+d_{Iprs}^{\mathrm{nsep,ex}})(Ap|rs)^{\mathrm{RI}}], \tag{19}$$

where we have introduced the excited state densities

$$D_{pq}^{F,\mathrm{ex}}=D_{pq}^{F,\xi}+D_{pq}^{F,A}, \tag{20}$$

$$d_{pqrs}^{\mathrm{nsep,ex}}=d_{pqrs}^{\mathrm{nsep},\xi}+d_{pqrs}^{\mathrm{nsep},A}. \tag{21}$$

Note, that the two-particle density in the MO basis has been used (see above).

The first derivative of the excited state energy with respect to an external perturbation x can now be calculated from an expression which is completely analogous to the ground state gradient

$$\frac{dL}{dx}=\sum_{\alpha\beta}D_{\alpha\beta}^{\mathrm{eff,ao}}h_{\alpha\beta}^{[x]}+\tfrac{1}{2}\sum_{\alpha\beta\gamma\delta}d_{\alpha\beta\gamma\delta}^{\mathrm{sep,ao}}(\alpha\beta|\gamma\delta)^{[x]}$$
$$-\sum_{\alpha\beta}F_{\alpha\beta}^{\mathrm{eff,ao}}S_{\alpha\beta}^{[x]}+\sum_{\alpha\beta P}\Delta_{\alpha\beta}^{\mathrm{ao},P}(\alpha\beta|P)-\sum_{PQ}\gamma_{PQ}V_{PQ}^{[x]}, \tag{22}$$

where the effective (or relaxed) one-particle density is defined as

$$D_{\alpha\beta}^{\mathrm{eff,ao}}=\sum_{pq}C_{\alpha p}C_{\beta q}D_{pq}^{\mathrm{eff}}, \tag{23}$$

$$D_{pq}^{\mathrm{eff}}=D_{pq}^{\mathrm{SCF}}+D_{pq}^{F,\xi}+D_{pq}^{F,A}+\tfrac{1}{2}(\overline{\kappa}_{pq}+\overline{\kappa}_{qp}). \tag{24}$$

The separable part of the two-electron density has a very simple structure

$$d_{\alpha\beta\gamma\delta}^{\mathrm{sep,ao}}=\mathcal{S}_{\gamma\delta}^{\alpha\beta}(1-\tfrac{1}{2}\mathcal{P}_{\beta\delta})(D_{\alpha\beta}^{\mathrm{eff,ao}}-\tfrac{1}{2}D_{\alpha\beta}^{\mathrm{SCF,ao}})D_{\gamma\delta}^{\mathrm{SCF,ao}} \tag{25}$$

and is constructed on-the-fly during the contraction with the derivatives of the electron repulsion integrals. Here, $\mathcal{S}_{\gamma\delta}^{\alpha\beta}$ symmetrizes a function according to $\mathcal{S}_{\gamma\delta}^{\alpha\beta}f_{\gamma\delta}^{\alpha\beta}=f_{\gamma\delta}^{\alpha\beta}+f_{\delta\gamma}^{\beta\alpha}$ and $\mathcal{P}_{\alpha\beta}$ denotes a permutation operator which interchanges two indices.

The nonseparable part of the two-electron density is contracted with two- and three-index electron repulsion integrals to the intermediates

$$\Delta_{\alpha\beta}^{\mathrm{ao},P}=\sum_{pq}\Lambda_{\alpha p}^{p}\Lambda_{\beta q}^{h}\sum_{rsQ}\hat{d}_{pqrs}^{\mathrm{nsep,ex}}(rs|\hat{Q})V_{PQ}^{-1} \tag{26}$$

and

$$\gamma_{PQ}=\sum_{\alpha\beta R}(\alpha\beta|R)\Delta_{\alpha\beta}^{\mathrm{ao},P}V_{RQ}^{-1}. \tag{27}$$

The latter term occurs in the gradient expression since also the auxiliary basis depends on the nuclear coordinates which gives rise to a contribution from the first derivative of the metric matrix V_{PQ}. A similar contribution from the overlap matrix of the one-electron basis is contracted with an effective Fock matrix, which can be expressed as

$$F_{\alpha\beta}^{\mathrm{eff,ao}}=\tfrac{1}{2}\sum_{pq}C_{\alpha p}C_{\beta q}(D_{pq}^{\mathrm{eff}}+D_{qp}^{\mathrm{eff}})\epsilon_q$$
$$+\sum_{Ip}C_{\alpha I}C_{\beta q}\sum_{rs}(D_{rs}^{F,\mathrm{ex}}+\overline{\kappa}_{rs})A_{rsIq}$$
$$+\tfrac{1}{2}\sum_{pq}C_{\alpha p}C_{\beta q}\sum_{rst}(d_{rstp}^{\mathrm{nsep,ex}}+d_{rspt}^{\mathrm{nsep,ex}})(rs|tq)^{\mathrm{RI}}. \tag{28}$$

Note that, similar to the expression for η_{AI}^{κ}, the above expression employs the two-particle densities in the MO representation.

C. Triplet excited states

First-order properties and energy gradients for triplet excited states within the coupled-cluster framework have previously been reported for spin–orbital based approaches, see, e.g., Ref. 42. An explicitly spin-coupled basis for a more efficient evaluation of triplet excited states within coupled-cluster theory has been developed by Hald *et al.*[43–47] In particular, the evaluation of first-order properties for triplet excited states was presented in Ref. 46. Within the triplet-coupled basis, the expressions obtained for the Jacobian transformations and the **B**-matrix transformation resemble very much those for the singlet case.

For the triplet gradient expression, only the A-type densities (11) and (14) are subject to some minor changes. These are indicated in the respective tables of the supplementary information.[40] The Lagrange multipliers $\overline{t}$ and $\overline{\kappa}$ still possess singlet symmetry and are only indirectly affected via the inhomogeneities of the corresponding response equations which are subject to minor changes emerging from the **B**-matrix transformation [cf. Eq. (15)] and the densities $D^{F,A}$ and $d^{\mathrm{nsep},A}$ [cf. Eq. (19)]. Details on the **B**-matrix transformation with triplet adapted right and left eigenvectors are described in Ref. 46.

We recall that for CC2 both right and left excitation vectors can be written as a sum of the symmetric and the antisymmetric part with respect to an interchange of the index pairs (ai) and (bj):

$${}^{3}R_{ij}^{ab}=\tfrac{1}{2}({}^{(+)}R_{ij}^{ab}+{}^{(-)}R_{ij}^{ab}), \tag{29}$$

$${}^{(+)}R_{ij}^{ab}={}^{(+)}R_{ji}^{ba}=-{}^{(+)}R_{ij}^{ba}, \tag{30}$$

$${}^{(-)}R_{ij}^{ab}=-{}^{(-)}R_{ji}^{ba}\neq{}^{(-)}R_{ij}^{ba}. \tag{31}$$

This reflects the symmetries of the underlying operator basis.[43] Therefore, the expression for the doubles contribution (cf. Ref. 40) to the excited state one-particle density has to be calculated according to

$$\sum_{abk}{}'L_{jk}^{ab}R_{ik}^{ab}=\tfrac{1}{2}\sum_{abk}{}^{(+)}L_{jk}^{ab}{}^{(+)}R_{ik}^{ab}+\sum_{abk}{}^{(-)}L_{jk}^{ab}{}^{(-)}R_{ik}^{ab}, \tag{32}$$

$$\sum_{ijc}{}'L_{ij}^{ac}R_{ij}^{bc}=\tfrac{1}{2}\sum_{ijc}{}^{(+)}L_{ij}^{ac}{}^{(+)}R_{ij}^{bc}+\sum_{ijc}{}^{(-)}L_{ij}^{ac}{}^{(-)}R_{ij}^{bc}, \tag{33}$$

where the prime indicates a restricted summation.

Downloaded 13 Feb 2004 to 141.52.232.84. Redistribution subject to AIP license or copyright, see http://jcp.aip.org/jcp/copyright.jsp

Pass 1

loop IJ-blocks

calculate $\bar{t}_{ij}^{ab}$ and t_{ij}^{ab} for $i,j \in I,J$

increment $D_{ab}^{F,\xi} += \sum_{ijc} \bar{t}_{ij}^{ac} t_{ij}^{bc}$

increment Y-type intermediates, e.g. $\tilde{Y}_{ia}^{Q} += \sum_{bj} (2t_{ij}^{ab} - t_{ij}^{ba}) \breve{B}_{jb}^{Q}$

increment C-type intermediates, e.g. $\tilde{C}_{ia} += \sum_{bj} (2t_{ij}^{ab} - t_{ij}^{ba}) \bar{t}_{j}^{b}$

end loop IJ-blocks

loop AB-blocks

calculate $\bar{t}_{ij}^{ab}$ and t_{ij}^{ab} for $a,b \in A,B$

increment $D_{ij}^{F,\xi} += \sum_{abk} \bar{t}_{ik}^{ab} t_{jk}^{ab}$

end loop AB-blocks

complete ${}^{\xi}\Gamma$ intermediates according to Table V of supplement.

form ${}^{\xi}\Omega$ and ${}^{\xi}H$ intermediates according to Table VI of supplement.

Pass 2

loop IJ-blocks

calculate $\bar{E}_{ij}^{ab}$ and E_{ij}^{ab} for $i,j \in I,J$

increment $D_{ab}^{F,A} += \sum_{ijc} \bar{E}_{ij}^{ac} E_{ij}^{bc}$

increment Y-type intermediates, e.g. $\tilde{Y}_{ia}^{Q} += \sum_{bj} (2E_{ij}^{ab} - E_{ij}^{ba}) \bar{B}_{jb}^{Q}$

increment C-type intermediates, e.g. $\tilde{C}_{ia} += \sum_{bj} (2E_{ij}^{ab} - E_{ij}^{ba}) \bar{E}_{j}^{b}$

end loop IJ-blocks

loop AB-blocks

calculate $\bar{E}_{ij}^{ab}$ and E_{ij}^{ab} for $a,b \in A,B$

increment $D_{ij}^{F,A} += \sum_{abk} \bar{E}_{ik}^{ab} E_{jk}^{ab}$

end loop AB-blocks

complete ${}^{A}\Gamma$ intermediates according to Table V of supplement.

form ${}^{A}\Omega$ and ${}^{A}H$ intermediates according to Table VI of supplement.

FIG. 1. Schematic algorithm for calculation of excited state densities. It illustrates how both ξ and A type intermediates can be calculated using the same subroutines. Refer also to the supplement (Ref. 40) for explicit expressions.

III. IMPLEMENTATION

The excited state gradient has been implemented in the RICC2 module of the TURBOMOLE program package. The central new quantity which has to be computed is the RI two-particle density $\Delta_{\alpha\beta}^{\mathrm{ao},Q}$. As stated in Ref. 34 for the ground state gradient, the storage of $\Delta_{\alpha\beta}^{\mathrm{ao},Q}$ on disk or in memory is not desirable. Noting, that for triple-ζ basis sets typically the number of active occupied orbitals is only a 10th (or less) of the number of basis functions, it is more efficient to express the two-particle density by seven (five, if the intermediates grouped together in brackets are only stored as sum) three-index intermediates having one active occupied index, and the appropriate transformation matrices

$$\Delta_{\alpha\beta}^{\mathrm{ao},Q} = \sum_{j} \; (C_{\alpha j}({}^{\xi}\Gamma_{j\beta}^{(a),Q} + {}^{A}\Gamma_{j\beta}^{(a),Q}) + ({}^{\xi}\Gamma_{j\alpha}^{(b),Q} + {}^{A}\overline{\Gamma}_{j\alpha}^{(b),Q})\Lambda_{\beta j}^{h} + {}^{A}\Gamma_{j\alpha}^{(b),Q}\overline{\Lambda}_{\beta j}^{h} + \breve{\Lambda}_{\alpha j}^{p}(\overline{t})\,{}^{\xi}\Gamma_{j\beta}^{(c),Q} + \breve{\Lambda}_{\alpha j}^{p}(\overline{E})\,{}^{A}\Gamma_{j\beta}^{(c),Q}). \tag{34}$$

In addition we use two intermediates, ${}^{\mathrm{ex}}H$ and ${}^{\mathrm{ex}}\Omega$, from which the effective Fock matrix, Eq. (28), and the inhomogeneity for the CPHF equations, Eq. (19), can be evaluated as

$$F_{\alpha\beta}^{\mathrm{eff,ao}} = \sum_{pq} \; C_{\alpha p} C_{\beta q} \tfrac{1}{2}(D_{pq}^{\mathrm{eff}} + D_{qp}^{\mathrm{eff}})\epsilon_q \sum_{Ip} \; C_{\alpha I} C_{\beta q} \sum_{rs} \; (D_{rs}^{F,\mathrm{ex}} + \overline{\kappa}_{rs})A_{rsIq} + \tfrac{1}{2}\sum_{pq} \; C_{\alpha p} C_{\beta q}({}^{\mathrm{ex}}H_{pq} + {}^{\mathrm{ex}}\Omega_{qp}), \tag{35}$$

$$\eta_{AI}^{\kappa,f} = \tfrac{1}{2}(D_{AI}^{F,\mathrm{ex}} + D_{IA}^{F,\mathrm{ex}})(\epsilon_I - \epsilon_A) - \tfrac{1}{4}\sum_{pq} \; (D_{pq}^{F,\mathrm{ex}} + D_{qp}^{F,\mathrm{ex}})A_{pqAI} + ({}^{\mathrm{ex}}H_{AI} - {}^{\mathrm{ex}}\Omega_{AI} - {}^{\mathrm{ex}}H_{IA} + {}^{\mathrm{ex}}\Omega_{IA}). \tag{36}$$

Explicit expressions for the Γ-type intermediates and ${}^{\mathrm{ex}}\Omega^{(x)}$ and ${}^{\mathrm{ex}}H^{(x)}$ are given in Ref. 40. The scheme to calculate the excited state gradient can be summarized as follows.

(i) First the ground state equations are solved for t and the excitation vectors $\overline{E}$ and E as well as the Lagrange multipliers $\overline{t}$ are determined. This is done using the algorithms described in previous communications.[32,33] These take full advantage of the doubles-direct formulation, i.e., they avoid the storage of four-index intermediates on disk or in memory and instead recalculate them from three-index quantities whenever needed.

(ii) The calculation of the one-particle and the RI-two-particle densities is organized in two passes: First all ξ-type intermediates and after that all A-type intermediates are calculated, where both times the same program modules are used (the same routines serve also for calculating the ground state gradient as the ground state intermediates are only special cases of the ξ intermediates). A sketch of the algorithm is presented in Fig. 1.

(iii) After completion of the ξ- and A-type intermediates, the right-hand side for the CPHF equations is set up according to Eq. (36) and the CPHF equations are solved using an integral direct algorithm. After that the density D^{eff} and the effective Fock matrix F^{eff} are constructed.

(iv) Finally the gradient expression Eq. (22) is evaluated using the same algorithm as for the ground state.[34] The separable two-particle density $d_{\alpha\beta\gamma\delta}^{\mathrm{sep,ao}}$ is constructed on-the-fly for a fixed AO shell quadruple and contracted with the derivatives of the conventional two-electron integrals. The RI two-particle density $\Delta_{\alpha\beta}^{\mathrm{ao},P}$ is constructed according to Eq. (34) in a batched loop over β and contracted with the derivatives of the RI three-center integrals.

Downloaded 13 Feb 2004 to 141.52.232.84. Redistribution subject to AIP license or copyright, see http://jcp.aip.org/jcp/copyright.jsp

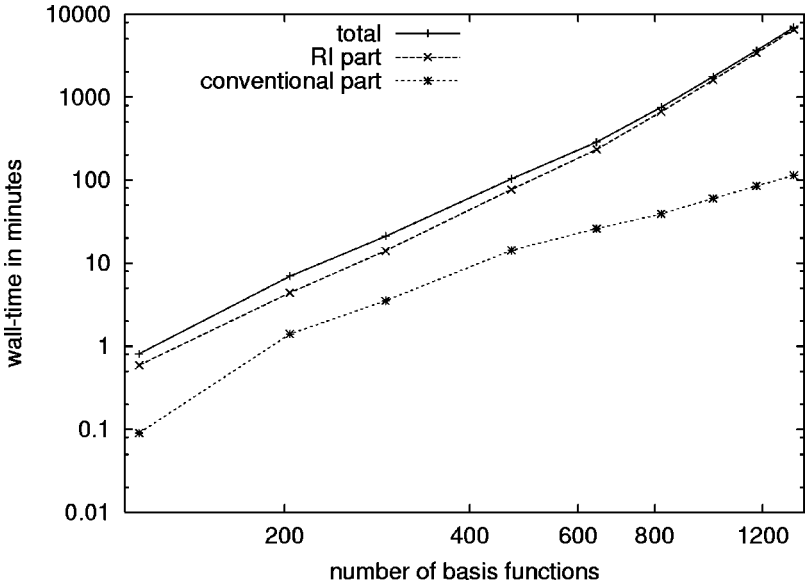


FIG. 2. Double-logarithmic plot illustrating the scaling behavior of RI and conventional part for the polyenes C_nH_{n+2} ($n=2$, 4, 6, 10, 14, 18, 22, 26, 30). For each molecule, the gradient of the $1\,^1B_u$ state was calculated using the cc-pVTZ basis set. Given are wall times obtained on one Intel P4 node (2.4 GHz, 4GB RAM). The C_{2h} point-group symmetry was exploited and the core memory usage was restricted to 1 GB.

IV. PERFORMANCE AND ACCURACY OF CC2 FOR EXCITED STATES

A. Timings for ground and excited state gradients

The performance of the T_2-direct CC2 approach using the RI approximation has already been reported previously.[33] Compared to a conventional disk-based approach, it turns out to be already efficient for small systems (triatomic molecules with double-ζ basis sets) even though it recalculates the doubles amplitudes several times. As the molecular systems grow larger and basis sets of triple-ζ or even higher quality are employed, it clearly outperforms the conventional implementation.

In order to test the applicability and the stability of the program for large systems, gradient calculations were run for a series of polyenes (C_nH_{n+2}, $n=2$, 4, 6, 10, 14, 18, 22, 26, 30), using a basis set of triple-ζ quality (cc-pVTZ). The elapsed times for single point calculations at the MP2 ground state structure are plotted in a double-logarithmic diagram, Fig. 2. The largest example comprises 152 correlated electrons, 1348 basis functions and 3390 auxiliary basis functions. A system of that size still proves to be feasible, though the total computation time for the gradient is nearly five days on an Intel P4 system (compare caption of Fig. 2). The elapsed time is solely determined by the CPU performance, no major I/O bottlenecks are observed. The mass storage requirement is about 30 GB; for comparison: a conventional implementation would roughly need as much as 18 GB to store the doubles part of *one* excitation vector.

For the largest cases an effective scaling of about $\mathcal{O}(N^{4.5})$ is found. The computation times of the smaller polyenes are governed by lower-scaling parts (integral transformations and steps involving conventional four-index integrals), e.g., between C_6H_8 and $C_{10}H_{12}$ the effective scaling is $\mathcal{O}(N^{3.4})$. Due to the topology of the polyenes, integral prescreening is very effective for the four-index integrals, i.e., the solution of the CPHF equations and the four-index integral gradient. The scaling for this part drops to $\mathcal{O}(N^2)$ for the larger cases and therefore contributes only with 2% to the total runtime for $C_{30}H_{32}$. At variance, for medium sized and/or less favorably shaped molecules, we observe that a relatively large part of the computation time is consumed by the calculation of four-index integrals, e.g., 20% for C_6H_8. This is even more pronounced in calculations with diffuse basis sets, e.g., in a calculation on benzene with a aug-cc-pVTZ basis set we found that more than 50% of the computation time is due to these steps. To overcome this imbalance a combination with the recently published RI–SCF[48] procedure appears highly desirable.

B. Accuracy of the RI approximation

Naturally, the RI approximation introduces an additional source of error (hereafter denoted as RI error). The RI error has already been studied very carefully in the case of RI–MP2.[39,49,50] It was established that the RI error basically behaves like the conventional one-electron basis set error, i.e., it varies smoothly and exhibits global consistency.[49] The RI error can be kept small compared to basis set and correlation errors if auxiliary basis sets are optimized, thereby retaining an economic size of the latter. In a series of preceding communications, we have addressed the RI error for vertical excitation energies, transition moments, excited state first-order response properties,[33] as well as for ground state structure parameters.[34] It was found that for CC2, similar as for MP2, the RI error is nearly two orders in magnitude smaller than the one-electron basis set error and thus is negligible in any practical application.

At this place, it did not appear necessary to carry out another large scale study for the gradient code as calculations with conventional electron repulsion integrals are rather time consuming. Instead, the influence of the RI approximation is demonstrated for a few sample molecules, for which we calculated adiabatic excitation energies and structure constants with both a conventional implementation (ACESII[51]) and the present RI code. The aug-cc-pVTZ basis set was used and all electrons were correlated, since the conventional code does

Downloaded 13 Feb 2004 to 141.52.232.84. Redistribution subject to AIP license or copyright, see http://jcp.aip.org/jcp/copyright.jsp

TABLE I. RI error in excited state bond lengths and angles of selected molecules. The aug-cc-pVTZ basis set was used, all electrons were correlated. The error is defined as $\Delta^{RI}=x^{RI}-x$, where x is the respective quantity under consideration. The excitation energies are given in eV, lengths and angles are quoted in pm and degrees, respectively.

		T_e		Structure		
Molecule	State	RI-CC2	Δ^{RI}	Parameter	RI-CC2	Δ^{RI}
BH	$1\,^1\Pi$	2.813	−0.000 26	r_e	119.97	0.000
BF	$1\,^1\Pi$	6.378	−0.000 19	r_e	131.59	0.001
	$1\,^3\Pi$	3.399	−0.000 27	r_e	132.15	0.001
CO	$1\,^1\Pi$	7.983	−0.000 08	r_e	128.64	0.002
SiF_2	$1\,^1B_1$	5.511	−0.000 07	d(SiF)	162.85	0.000
				∠(FSiF)	115.85	−0.032
CCl_2	$1\,^1B_1$	2.080	−0.000 63	d(CCl)	164.21	−0.006
				∠(ClCCl)	132.72	−0.023
HCN	$1\,^1A''$	6.869	+0.000 16	d(CH)	110.88	0.013
				d(CN)	131.70	0.036
				∠(HCN)	122.31	−0.329
HCP	$1\,^1A''$	4.572	+0.000 18	d(CH)	108.27	0.000
				d(CP)	171.07	−0.005
				∠(HCP)	129.30	0.017
C_2H_2	$1\,^1A_u$	5.454	+0.000 15	d(CH)	108.63	0.000
				d(CC)	137.70	0.005
				∠(HCC)	121.97	−0.013
CH_2O	$1\,^1A''$	3.621	−0.000 29	d(CH)	108.46	−0.011
				d(CO)	135.28	0.011
				∠(HCH)	121.35	0.101
				ϕ	25.87	−0.330
CH_2S	$1\,^1A_2$	2.224	−0.000 30	d(CH)	107.87	0.001
				d(CS)	170.22	−0.003
				∠(HCH)	120.59	0.000

not support the frozen-core approximation in gradient calculations. The results are listed in Table I.

As for vertical excitation energies, the RI error in adiabatic excitation energies is very small: for all cases of the test set it is well below 1 meV. Though it may slightly increase for molecules with more extended chromophores,[32] it is expected not to exceed the range of 10–50 meV.

Similarly, the errors in the structure parameters caused by the RI approximation are small. In our test set we find errors below 0.1 pm for bond lengths and at most 0.33 degrees for angles. We note that, compared to the RI error in the ground state structures, these errors are larger by a factor of about 10. We conjecture that these errors are mainly due to integrals of the type $(ab|ij)$ which contribute a large part to the excitation energy but may not be fitted optimally as the optimization procedure for auxiliary basis sets focuses on $(ai|bj)$ type integrals.[50] This hypothesis still needs to be tested. In our opinion, however, the RI error obtained with the current auxiliary basis sets is small enough to be neglected in applications.

C. Performance of CC2 for excited state properties

In a previous communication,[34] we have already studied the accuracy of CC2 in ground state calculations. Structures and vibrational frequencies of a set of molecules were calculated using CC2 and MP2 analytic gradient codes. Results at the CCSD(T) level were used as reference. As expected, CC2 has an accuracy comparable to MP2. Some shortcomings, however, were found for triple bonds, which are too long at the CC2 level by about 2–3 pm. The corresponding vibrational frequencies are too weak by about 100–200 cm^{-1}. On the other hand, CC2 performs slightly better than MP2 for molecules with many lone-pairs. Here, MP2 typically yields too short bonds and too strong force constants.

Unfortunately, it is at present not feasible to set up a similar test set for excited states and to compare CC2 results with a highly correlated method. Gradient codes are only available for CCSD, whereas at least triples corrected methods like CC3 would be necessary to obtain reliable results to compare with. Some high-level results for diatomic molecules are available from the literature,[52] but for polyatomic molecules evaluation of the structures using numerical gradients is rather tedious and computationally expensive. Therefore we adopted in large parts the test set used by Furche and Ahlrichs for assessing a TDDFT gradient code.[13] The test set consists of molecules, for which presumably accurate experimental data exists. We restricted the present study to molecules with a closed shell ground state and removed molecules like BeO, which are multiple reference cases and not suited for CC2. The reduced set consists of 20 molecules with 2–6 atoms.

As argued in Ref. 13, extensive statistics are not suitable for evaluating the results, as the outcome strongly depends on the choice of the test molecules. Above that, many uncertainties arise since the experimental 0–0 transitions, structure parameters and vibrational frequencies of polyatomic molecules are not corrected for anharmonicities, which on the theoretical side are very costly to incorporate. Even though

Downloaded 13 Feb 2004 to 141.52.232.84. Redistribution subject to AIP license or copyright, see http://jcp.aip.org/jcp/copyright.jsp

for diatomic molecules such corrected values are available, it has to be kept in mind that these numbers are no observables but fit parameters of a model Hamiltonian. Again, a more accurate comparison with experiment could only be made by simulating the spectra and including higher-order corrections to the forcefield, which would be costly and beyond the scope of the present investigation. Here, we rather aim at testing the applicability of the method, i.e., which types of molecules and excited states are described well and for which cases is CC2 not appropriate.

(a) Computational procedure: All calculations were carried out with the RI–CC2 code described in the previous sections. The correlation-consistent basis sets aug-cc-pVXZ (X=D, T, Q) of Dunning and co-workers[53,54] were employed, with exception of the Rydberg state of water for which triply augmented basis sets (t-aug-cc-pVXZ) were used. For lithium and magnesium only the basis sets cc-pVXZ are available. For these elements we constructed aug-cc-pVTZ-like basis sets by adding diffuse functions with exponents obtained by even-tempered extrapolation of the two smallest exponents in the cc-pVTZ basis. Corresponding auxiliary basis sets were optimized using the procedure described in Refs. 39 and 50. The diffuse exponents and the auxiliary basis sets are given in Ref. 40. These auxiliary basis sets were also used for calculations in the aug-cc-pVDZ basis, whereas we desisted from calculations with quadruple-ζ basis sets for these elements. Structures were converged to an internal gradient norm of $10^{-3}E_H/a_0$, force constants were obtained by numerical differentiation (central differences in Cartesian coordinates with an increment of $0.01a_0$).

(b) Diagnostics: Criteria which allow to decide whether a method is adequate for a certain system are important tools for the interpretation of calculated data. For coupled-cluster ground states, Janssen and Nielsen[55,56] have proposed two diagnostics,

$$D_1 = \sqrt{\max\left(\lambda_{\max}\left[\sum_i t_{ai}t_{bi}\right], \lambda_{\max}\left[\sum_a t_{ai}t_{aj}\right]\right)} \tag{37}$$

and

$$D_2 = \sqrt{\max\left(\lambda_{\max}\left[\sum_{ijc} t_{ij}^{ac}t_{ij}^{bc}\right], \lambda_{\max}\left[\sum_{kab} t_{ik}^{ab}t_{jk}^{ab}\right]\right)}, \tag{38}$$

where $\lambda_{\max}[\mathbf{M}]$ is the largest eigenvalue of a positive definite matrix $\mathbf{M}$. In connection with CC2, these diagnostics have already been discussed in Ref. 34.

To be well described at the CC2 level, excited states must be dominated by single-excitations out of the ground state wave function. For this purpose we suggested recently[46] the percent contribution of the single excitation part to the total biorthogonal norm of the excitation vectors E and $\overline{E}$,

$$\%\langle \overline{E}_1 | E_1 \rangle = \sum_{\nu_1} \overline{E}_{\nu_1} E_{\nu_1} \langle \nu_1 | \tau_{\nu_1} | \mathrm{HF} \rangle \times 100\%. \tag{39}$$

This definition has the advantage of being independent of the choice of the excitation operator basis.

The resulting diagnostics for the molecules in our test set are summarized in Table II. We list the values obtained from the above expressions at the equilibrium geometry of the excited state as obtained in the aug-cc-pVTZ basis set. In Refs. 55 and 56 the authors give values of 0.04 (0.05) for D_1 and 0.17 (0.18) for D_2 which in the case of MP2 (CCSD) should not be exceeded, to obtain reliable results. Considering, however, that (a) for excited states we certainly enter more difficult regions of the nuclear configuration space and (b) that we in general do not expect highly accurate results from a second-order method like CC2, these bounds are too strict for our purposes. To our experience, results will be still acceptable up to values of 0.10 to 0.15 for D_1 and 0.2 to 0.25 for D_2, whereas higher values indicate a breakdown of the method. In addition, $\%\langle \overline{E}_1 | \overline{E}_1 \rangle$ should be larger than 85%. These diagnostics can of course only assist the interpretation of results and do not replace the understanding of the chemistry.

TABLE II. Measures of the quality of the CC2 wave function obtained with the aug-cc-pVTZ basis set at the optimized structures. The D_1 and D_2 measures assess the quality of the ground-state wave function. The biorthogonal norm $\langle \overline{E_1} | E_1 \rangle$ gives the percentage of single-excitation contribution to the excitation. For the exact definition see Sec. IV.

Molecule	State	D_1	D_2	$\langle \overline{E_2} \vert E_2 \rangle$
Li_2	$1\,^1\Sigma_u^+$	0.0212	0.1873	93.6
BH	$1\,^1\Pi$	0.0163	0.1495	97.4
BF	$1\,^1\Pi$	0.0458	0.1463	96.7
	$1\,^3\Pi$	0.0459	0.1466	98.8
	$1\,^3\Sigma^+$	0.0381	0.1443	97.7
N_2	$1\,^3\Pi_g$	0.0470	0.2101	94.7
	$1\,^1\Sigma_u^-$	0.0539	0.2268	97.1
	$1\,^1\Pi_g$	0.0491	0.2151	92.9
	$1\,^1\Delta_u$	0.0524	0.2232	96.8
CO	$1\,^1\Pi$	0.0948	0.1919	93.8
	$1\,^3\Pi$	0.0742	0.1766	96.9
Mg_2	$1\,^1\Sigma_u^+$	0.0250	0.1886	95.3
SiO	$1\,^1\Pi$	0.1812	0.2464	85.8
	$1\,^3\Delta$	0.2600	0.3049	86.9
H_2O[a]	$2\,^1B_1$	0.0318	0.1276	90.6
SO_2	$1\,^3B_1$	0.1229	0.2625	91.2
SiF_2	$1\,^1B_1$	0.0596	0.1536	94.8
CCl_2	$1\,^1B_1$	0.0874	0.1523	94.9
CS_2	$1\,^3A_2$	0.0937	0.2221	92.1
HCN	$1\,^1A''$	0.1312	0.2302	96.5
HCP	$1\,^1A''$	0.1416	0.2386	95.7
NH_3	$1\,^1A_2''$	0.0228	0.1284	89.3
C_3	$1\,^1\Pi_u$	0.0803	0.2227	93.4
C_2H_2	$1\,^1A_u$	0.0522	0.2366	96.6
CH_2O	$1\,^1A''$	0.0796	0.2067	91.6
	$1\,^3A''$	0.0723	0.2057	93.1
CH_2S	$1\,^1A_2$	0.0746	0.1998	92.9
	$1\,^3A''$	0.0697	0.1980	94.3
trans-$(CHO)_2$	$1\,^1A_u$	0.0670	0.1973	91.6
HC_2CHO	$1\,^1A''$	0.1155	0.2290	88.6

[a]The t-aug-cc-pVTZ basis set was used.

(c) Excitation energies: For diatomic molecules adiabatic excitation energies T_e were computed, since for those experimental estimates exist. For all other molecules 0–0 transition energies were calculated using the harmonic approximation. Anharmonicities should influence the results little as only the differences between the ground and the excited states enter. The results are listed in Tables III and IV.

The double-ζ basis gives for most cases qualitatively correct results, though for a number of molecules it turns out

Downloaded 13 Feb 2004 to 141.52.232.84. Redistribution subject to AIP license or copyright, see http://jcp.aip.org/jcp/copyright.jsp

TABLE III. Adiabatic excitation energies T_e (eV) of diatomic molecules calculated with RI–CC2 using different basis sets. The experimental values are taken from Ref. 71.

Molecule	State	aug-cc-pVDZ	aug-cc-pVTZ	aug-cc-pVQZ	Expt.
Li_2	$1\,^1\Sigma_u^+$	1.90	1.91		1.74
		(1.91)[a]	(1.92)[a]		
BH	$1\,^1\Pi$	2.87	2.83	2.82	2.87
BF	$1\,^1\Pi$	6.38	6.38	6.37	6.34
	$1\,^3\Pi$	3.25	3.39	3.42	3.61
	$1\,^3\Sigma^+$	7.56	7.54	7.55	7.57
N_2	$1\,^3\Pi_g$	7.12	7.25	7.29	7.39
	$1\,^1\Sigma_u^-$	8.56	8.65	8.69	8.45
	$1\,^1\Pi_g$	8.29	8.35	8.38	8.59
	$1\,^1\Delta_u$	9.22	9.31	9.35	8.94
CO	$1\,^1\Pi$	7.91	7.93	7.96	8.07
	$1\,^3\Pi$	5.95	6.03	6.07	6.04
Mg_2	$1\,^1\Sigma_u^+$	3.25	3.21		3.23
		(3.24)[a]	(3.16)[a]		
SiO	$1\,^1\Pi$	4.65	4.74	4.77	5.31
	$1\,^3\Delta$	3.47	3.71	3.78	4.52

[a]Values in parentheses refer to calculations with correlated $1s$ shell (lithium) or correlated $2s2p$ shell (magnesium), respectively.

to be too inflexible. The deviations from the excitation energies obtained with aug-cc-pVQZ are between 0.1 and 0.3 eV, whereas results obtained with triple-ζ basis sets deviate by less than 0.1 eV. This stresses clearly the well-known fact that triple-ζ basis sets are most appropriate for second-order correlation methods. The same observation applies for all other properties investigated.

Comparing calculated and experimental excitation energies CC2 proves to be very reliable. Most deviations fall into a range of ± 0.3 eV. Larger deviations are only found for SiO (-0.7 eV) and the Rydberg state of water (-0.8 eV). SiO clearly is a difficult case with considerable multireference character, as indicated by large values for D_1 (>0.18) and D_2 (>0.25). Above that, the excited states exhibit large double excitation contributions. For water, the large deviation is somewhat unexpected, since the D_1 and D_2 diagnostics are small, even in the sense of the strict bounds of Refs. 55 and 56. Also the double-excitation character does not exceed 10%. In a previous study employing a modified aug-cc-pVDZ basis, however, vertical excitation energies of water deviated by -0.4 to -0.5 eV[57] from the full CI result. Furthermore it is known from other theoretical studies of vertical excitation energies that CC2 typically yields too low-lying Rydberg states.[31,58]

TABLE IV. 0–0 transitions of polyatomic molecules calculated with RI-CC2 in the harmonic approximation. The experimental values are taken from Ref. 71 unless otherwise noted.

Molecule	State	aug-cc-pVDZ	aug-cc-pVTZ	aug-cc-pVQZ	Expt.
H_2O[a]	$2\,^1B_1$	8.91	9.11	9.20	10.00
SO_2	$1\,^3B_1$	2.56	2.86	2.92	3.19
SiF_2	$1\,^1B_1$	5.46	5.49	5.49	5.34
CCl_2[b]	$1\,^1B_1$	2.24	2.13	2.11	2.14
CS_2	$1\,^3A_2$	3.17	3.27	3.29	3.25
HCN	$1\,^1A''$	6.55	6.68	6.72	6.48
HCP	$1\,^1A''$	4.43	4.45	4.48	4.31
C_3	$1\,^1\Pi_u$	3.09	3.09	3.09	3.06
C_2H_2	$1\,^1A_u$	5.09	5.29	5.33	5.23
CH_2O[c]	$1\,^1A''$	3.44	3.49	3.52	3.49
	$1\,^3A''$	2.93	3.01	3.05	3.12
CH_2S[c]	$1\,^1A_2$	2.13	2.13	2.15	2.03
	$1\,^3A''$	1.74	1.77	1.79	1.80
trans-$(CHO)_2$	$1\,^1A_u$	2.67	2.69	2.70	2.72
HC_2CHO	$1\,^1A''$	3.08	3.14	3.17	3.24

[a]The *t*-aug-cc-pV*X*Z basis sets were used.
[b]Experimental data taken from Ref. 72.
[c]Experimental data taken from Ref. 73.

(d) Structures: Results are displayed in Table V. When comparing with experimental bond lengths, uncertainties of about 0.5 pm have to be taken into account,[28,59] as the values for polyatomic molecules are not corrected for vibrational effects. We find that, as for ground states, CC2 has a tendency to overestimate bond lengths, in particular for triple bonds. For N_2 and CO excited state bond lengths are obtained too long by up to 5.5 pm. For HCN ($+2.4$ pm), HCP ($+2.6$ pm) and acetylene ($+0.6$ pm), the overestimation of the bond lengths is more moderate. Since the errors in the ground and excited state structure parameters have the same sign, the changes in the bond lengths are obtained with better accuracy; e.g., for HCN: $\Delta r^{\mathrm{CC2}}(\text{aug-cc-pVQZ}) = 15.0$ pm versus $\Delta r^{\mathrm{exp}} = 14.1$ pm.

Furthermore it is observed that CC2 calculations tend to overestimate the change in the carbon–oxygen bond of aldehydes after $\pi^* \leftarrow n$ excitations. For formaldehyde this bond is too long by about 3 pm for the $^1A''$ and $^3A''$ state, a similar result is found for thioformaldehyde. The carbonyl bond of propynal is even too long by 8 pm, which is not unexpected, because the diagnostics indicate for this case a (nearby) breakdown of the CC2 model.

The dimers of lithium and magnesium are difficult cases, since their potential energy curves are very shallow. Small changes in the energy have a huge effect on the structure. Taking this into account, CC2 gives a satisfying description of these molecules. Apart from that, another problem arises from the basis sets. The separation of the valence orbitals and the $1s$ shell of lithium (the $2s2p$ shell of magnesium, respectively) is too low to apply the frozen-core approximation to these inner shells. As a consequence, for the magnesium dimer the bond is too long if only the $3s$ electrons are correlated. Unfortunately, adequate tight polarization functions are missing to describe the inner-shell correlation effects in a well-tempered fashion: If we use the present basis sets, too short bonds arise due to basis set superposition effects.

It should be stressed, that CC2 provides in all considered cases a qualitatively correct description of the excited state structures—with the exception of the cumulene C_3 which has been forced by symmetry restriction to keep its high symmetry structure (cf. next paragraph). The planarity of the S_1 state of thioformaldehyde is correctly predicted, as well as the pyramidalization at the carbon atom in the T_1 state and in the excited states of formaldehyde. CC2 also describes properly the nonlinear excited state structures of acetylene, HCN and HCP and the planar structure of the S_1 state of propynal.

(e) Harmonic vibrational frequencies: Table VI lists the calculated vibrational frequencies as obtained from the har-

Downloaded 13 Feb 2004 to 141.52.232.84. Redistribution subject to AIP license or copyright, see http://jcp.aip.org/jcp/copyright.jsp

TABLE V. Excited state structure parameters (bond lengths in pm and angles in degrees) calculated with RI–CC2. For diatomic molecules, the experimental r_e values are quoted which are corrected for vibrational effects. Experimental values are taken from Refs. 71 and 74 unless otherwise noted.

Molecule	State	Parameter	aug-cc-pVDZ	aug-cc-pVTZ	aug-cc-pVQZ	Expt.
Li_2	$1\,^1\Sigma_u^+$	r_e	313.1	307.6		310.7
			(307.6)[a]	(307.5)[a]		
BH	$1\,^1\Pi$	r_e	122.7	121.0	120.9	121.9
BF	$1\,^1\Pi$	r_e	136.5	132.4	131.8	130.4
	$1\,^3\Pi$	r_e	136.5	132.9	132.3	130.8
	$1\,^3\Sigma^+$	r_e	125.7	123.0	122.4	121.5
N_2	$1\,^3\Pi_g$	r_e	126.8	125.6	125.1	121.3
	$1\,^1\Sigma_u^-$	r_e	132.2	131.1	130.7	127.6
	$1\,^1\Pi_g$	r_e	128.4	127.3	126.8	122.0
	$1\,^1\Delta_u$	r_e	131.0	129.9	129.5	126.8
CO	$1\,^1\Pi$	r_e	131.5	129.8	129.0	123.5
	$1\,^3\Pi$	r_e	124.8	123.6	123.0	120.6
Mg_2	$1\,^1\Sigma_u^+$	r_e	314.7	314.6		308.2
			(310.1)[a]	(305.1)[a]		
SiO	$1\,^1\Pi$	r_e	182.8	175.8	174.7	162.0
	$1\,^3\Delta$	r_e	188.6	185.8	185.2	171.5
H_2O[b]	$2\,^1B_1$	d(OH)	104.3	103.3	102.1	106.9
		∠(HOH)	102.6	102.1	103.2	101.6
SO_2	$1\,^3B_1$	d(SO)	162.9	156.4	155.4	149.4
		∠(OSO)	130.2	129.1	128.8	126.1
SiF_2[c]	$1\,^1B_1$	d(SiF)	168.4	163.5	162.8	160.1
		∠(FSiF)	116.8	116.2	115.9	115.9
CCl_2[c]	$1\,^1B_1$	d(CCl)	167.4	165.4	164.8	165.2
		∠(ClCCl)	131.1	132.0	132.0	131.4
CS_2	$1\,^3A_2$	d(CS)	167.1	165.4	164.9	164
		∠(SCS)	134.4	135.5	135.7	135.8
HCN	$1\,^1A''$	d(CH)	113.2	111.6	111.5	114.0
		d(CN)	133.9	132.4	132.1	129.7
		∠(HCN)	121.5	122.3	122.3	125.0
HCP	$1\,^1A''$	d(CP)	174.2	172.1	171.6	169
		∠(HCP)	125.6	128.0	128.4	128
C_3	$1\,^1\Pi_u$	d(CC)	134.6	132.6	132.2	130.5
C_2H_2[d]	$1\,^1A_u$	d(CC)	140.1	138.4	138.1	137.5
		d(CH)	110.7	109.3	109.2	110.5
		∠(HCC)	121.0	121.8	122.0	121.4
CH_2O[e]	$1\,^1A''$	d(CH)	110.0	108.8	108.7	109.8
		d(CO)	137.7	136.1	135.5	132.3
		∠(HCH)	122.0	121.6	121.6	118.4
		ϕ[f]	26.1	25.7	25.7	34.0
	$1\,^3A''$	d(CH)	110.5	109.3	109.2	108.4
		d(CO)	135.5	134.1	133.6	130.7
		∠(HCH)	118.3	117.9	118.0	121.8
		ϕ[f]	38.5	38.1	38.1	41.1
CH_2S[e]	$1\,^1A_2$	d(CH)	109.6	108.3	108.3	107.7
		d(CS)	172.8	171.1	170.6	168.2
		∠(HCH)	121.2	121.1	121.2	120.7
	$1\,^3A''$	d(CH)	109.5	108.3	108.2	108.2
		d(CS)	171.1	169.4	168.9	168.3
		∠(HCH)	120.7	120.6	120.5	119.3
		ϕ[f]	15.3	15.4	15.0	11.9
trans-$(CHO)_2$[g]	$1\,^1A_u$	d(CC)	149.2	148.0	147.9	146.0
		d(CH)	110.6	109.5	109.5	111.5
		d(CO)	127.0	125.8	125.4	125.2
		∠(HCC)	114.8	114.5	114.5	114
		∠(OCC)	123.8	123.9	123.9	123.7
HC_2CHO	$1\,^1A''$	d(C_1C_2)	125.8	123.9	123.8	123.8
		d(C_3H)	109.6	108.5	108.5	109.1
		d(C_3O)	143.0	141.2	140.6	132.5

[a]Values in parentheses refer to calculations with correlated 1*s* shell (lithium) or correlated 2*s*2*p* shell (magnesium), respectively.
[b]The *t*-aug-cc-pV*X*Z basis sets were used.
[c]Experimental values from Ref. 72.
[d]Experimental values from Ref. 75.
[e]Experimental values from Ref. 73.
[f]Out-of-plane angle of the oxygen or sulfur atom, respectively.
[g]Experimental values from Ref. 76.

Downloaded 13 Feb 2004 to 141.52.232.84. Redistribution subject to AIP license or copyright, see http://jcp.aip.org/jcp/copyright.jsp

TABLE VI. Harmonic vibrational frequencies (cm^{-1}) calculated with RI–CC2. For diatomic molecules, the experimental ω_e values are quoted which are corrected for anharmonicities. Experimental values are taken from Refs. 71 and 74 unless otherwise noted.

Molecule	State	Mode	aug-cc-pVDZ	aug-cc-pVTZ	aug-cc-pVQZ	Expt.
Li_2	$1\,^1\Sigma_u^+$	ω_e	269.8	275.9		255.5
			(279.0)[a]	(268.2)[a]		
BH	$1\,^1\Pi$	ω_e	2417.3	2458.0	2461.3	2250.9[b]
BF	$1\,^1\Pi$	ω_e	1049.6	1189.4	1204.5	1264.9
	$1\,^3\Pi$	ω_e	1162.5	1261.5	1270.4	1323.8
	$1\,^3\Sigma^+$	ω_e	1416.6	1565.1	1581.5	1629.3
N_2	$1\,^3\Pi_g$	ω_e	1411.6	1407.2	1425.4	1733.4
	$1\,^1\Sigma_u^-$	ω_e	1280.4	1283.0	1296.5	1530.3
	$1\,^1\Pi_g$	ω_e	1337.5	1327.2	1346.5	1694.2
	$1\,^1\Delta_u$	ω_e	1340.2	1341.1	1353.6	1559.3
CO	$1\,^1\Pi$	ω_e	1089.4	1138.1	1159.0	1518.2
	$1\,^3\Pi$	ω_e	1479.6	1516.3	1533.9	1743.4
Mg_2	$1\,^1\Sigma_u^+$	ω_e	182.8	180.9		190.6
			(191.3)[a]	(202.2)[a]		
SiO	$1\,^1\Pi$	ω_e	482.6	517.5	532.0	852.8
	$1\,^3\Delta$	ω_e	639.8	574.7	567.2	767
H_2O[c]	$2\,^1B_1$	$\nu_1(a_1)$	2872.2	2976.9	3077.0	3170
SO_2	$1\,^3B_1$	$\nu_1(a_1)$	480.3	650.5	673.3	905.7
		$\nu_2(a_1)$	221.2	275.3	285.0	359.8
SiF_2	$1\,^1B_1$	$\nu_1(a_1)$	613.4	686.0	705.2	598
		$\nu_2(a_1)$	208.4	228.8	234.6	342
CCl_2[d]	$1\,^1B_1$	$\nu_1(a_1)$	619.8	628.7	640.9	634.3
		$\nu_2(a_1)$	304.0	305.0	307.8	302.6
CS_2	$1\,^3A_2$	$\nu_1(a_1)$	682.1	675.8	682.0	691.5
		$\nu_2(a_1)$	259.3	243.0	243.4	310.8
HCN	$1\,^1A''$	$\nu_2(a')$	1309.3	1334.8	1344.9	1495.9
		$\nu_3(a')$	956.2	958.0	963.3	940.6
HCP	$1\,^1A''$	$\nu_2(a')$	852.5	879.9	888.0	950.9
		$\nu_3(a')$	680.5	635.7	636.1	566.6
C_3	$1\,^1\Pi_u$	$\nu_1(\sigma_g)$	1037.3	1060.2	1163.7	1085.9
		$\nu_2(\sigma_u)$	i666.7	i472.8	i762.3	
		$\nu_3(\pi_u)$	190.4	262.2	263.6	307.9
C_2H_2	$1\,^1A_u$	$\nu_2(a_g)$	1350.5	1362.6	1367.9	1385.0
		$\nu_3(a_g)$	1094.6	1086.3	1085.7	1047.6
CH_2O[e]	$1\,^1A''$	$\nu_1(a')$	3066.2	3064.9	3064.2	2846
		$\nu_2(a')$	1311.6	1323.1	1320.7	1293.1
		$\nu_3(a')$	969.6	1007.0	1014.6	1183
		$\nu_5(a'')$	3212.3	3200.1	3202.0	2968.3
		$\nu_6(a'')$	862.1	870.3	873.0	904
	$1\,^3A''$	$\nu_2(a')$	1285.0	1301.7	1297.8	1283.0
CH_2S[e]	$1\,^1A_2$	$\nu_1(a_1)$	3128.5	3128.1	3126.8	3034
		$\nu_2(a_1)$	1347.3	1342.0	1343.2	1316
		$\nu_3(a_1)$	779.6	791.3	798.8	820
		$\nu_4(b_1)$	3258.4	3251.0	3253.4	3081.3
		$\nu_5(b_1)$	776.6	768.5	769.4	799
	$1\,^3A''$	$\nu_2(a')$	1338.0	1338.0	1336.9	1320
		$\nu_3(a')$	829.0	839.1	846.0	859
trans-$(CHO)_2$[f]	$1\,^1A_u$	$\nu_1(a_g)$	3064.8	3054.3	3051.9	2809
		$\nu_2(a_g)$	1339.1	1363.9	1369.3	1391.4
		$\nu_3(a_g)$	1222.8	1233.5	1232.8	1195.2
		$\nu_4(a_g)$	1000.6	995.3	994.7	952.4
		$\nu_5(a_g)$	488.1	493.2	494.3	509.0
		$\nu_6(a_u)$	740.6	752.9	754.4	720.0
		$\nu_7(a_u)$	212.5	218.0	218.9	233.3
		$\nu_8(b_g)$	743.4	763.2	762.8	735.1
		$\nu_{10}(b_u)$	1207.9	1238.1	1248.0	1280.8
		$\nu_{11}(b_u)$	1140.7	1172.2	1176.4	1172
		$\nu_{12}(b_u)$	363.8	368.9	371.6	379.3
HC_2CHO[g]	$1\,^1A''$	$\nu_2(a')$	3183.1	3169.5	3170.0	2952.5
		$\nu_3(a')$	1873.7	1890.7	1898.2	1945.8
		$\nu_4(a')$	1202.4	1214.5	1217.7	1304.0
		$\nu_5(a')$	1066.9	1072.1	1074.1	1119.5
		$\nu_6(a')$	725.5	766.8	779.5	951.6
		$\nu_7(a')$	582.5	634.1	642.1	650
		$\nu_8(a')$	442.8	466.0	470.7	506.9
		$\nu_9(a')$	150.9	168.9	171.1	189.4
		$\nu_{10}(a'')$	518.0	547.2	550.2	462.1
		$\nu_{11}(a'')$	354.0	410.6	415.7	389.7
		$\nu_{12}(a'')$	108.6	313.3	323.9	345.9

[a]Values in parentheses refer to calculations with correlated $1s$ shell (lithium) or correlated $2s2p$ shell (magnesium), respectively.
[b]Benchmark calculations (CCSDT-3/cc-pV5Z, Ref. 52) result in 2374.
[c]The *t*-aug-cc-pV*X*Z basis sets were used.
[d]Experimental values from Ref. 72.
[e]Experimental values from Ref. 73.
[f]Experimental values from Ref. 77.
[g]Experimental values from Ref. 78. ν_4 and ν_6 are corrected for Fermi resonance.

Downloaded 13 Feb 2004 to 141.52.232.84. Redistribution subject to AIP license or copyright, see http://jcp.aip.org/jcp/copyright.jsp

TABLE VII. Excited state dipole moments calculated with CC2 in the unrelaxed and the relaxed formulation.

Molecule	State	aug-cc-pVDZ		aug-cc-pVTZ		aug-cc-pVQZ		Expt.
BH	$X\,^1\Sigma^+$	1.55	1.56	1.62	1.62	1.62	1.63	1.27[a]
	$1\,^1\Pi$	0.49	0.59	0.47	0.57	0.47	0.57	0.58[a]
CO	$X\,^1\Sigma^+$	−0.40	−0.26	−0.40	−0.27	−0.40	−0.28	−0.11[b]
	$1\,^1\Pi$	−0.29	0.04	−0.26	0.04	−0.22	0.05	0.34[b]
CH_2O	$X\,^1A_1$	2.27	2.40	2.27	2.38	2.33	2.38	2.33[c]
	$1\,^1A''$	1.11	1.79	1.09	1.74	1.10	1.73	1.56[c]
	$1\,^3A''$	1.06	1.47	1.06	1.45	1.08	1.46	1.29[c]
CH_2S	$X\,^1A_1$	1.67	1.74	1.64	1.71	1.66	1.72	1.65[c]
	$1\,^1A_2$	0.37	0.98	0.36	0.95	0.38	0.96	0.79[c]
	$1\,^3A''$	0.29	0.53	0.29	0.54	0.29	0.56	0.57[c]

[a]From Ref. 71.
[b]From Ref. 79. A minus sign implies a charge distribution C^-O^+.
[c]From Ref. 73.

monic force field. The quoted experimental frequencies of polyatomic molecules are not corrected for anharmonicities. Thus, the calculated harmonic frequencies are expected to lie in general slightly above the experimental fundamental frequencies.

The errors in the calculated harmonic frequencies are correlated with the deviations in the bond lengths. For N_2 and CO the too long bonds are accompanied by an underestimation of the vibrational frequencies by 200 to 360 cm^{-1}. For the remaining molecules with triple bonds only moderate deviations of around $-100\ cm^{-1}$ are found. As for bond lengths, the changes upon excitation are predicted rather accurately, e.g., for HCN: $\Delta\nu^{CC2}(\text{aug-cc-pVQZ}) = 618\ cm^{-1}$ versus $\Delta\nu^{exp} = 601\ cm^{-1}$.

For the cumulene C_3, we note that at the CC2 level adiabatic excitation energies and structure constants seem to match well, if no symmetry breaking is allowed. However, the force constant calculation reveals an imaginary frequency along the σ_u mode.

(f) Dipole moments: There exist only few accurate gas-phase measurements of excited state dipole moments. Thus only four examples are listed in Table VII. We also quote the ground state results, since these have not been investigated in the preceding communication, Ref. 34. Strikingly, for excited states somewhat larger differences occur between dipole moments calculated from the relaxed and the unrelaxed formulation of the Lagrange function (i.e., with and without including the contributions from orbital relaxation effects). The deviations amount to up to 0.6 debye for formaldehyde. An analysis of the calculations reveals that in all cases in the relaxed formulation the *electronic* contribution is smaller than in the unrelaxed approximation. The difference between relaxed and unrelaxed dipole moments is less pronounced for ground state dipole moments, which is not unexpected since here the T_1 amplitudes cover large parts of the orbital relaxation effects. Throughout, the relaxed dipole moments are closer to the experimental values.

(g) Comparison with CIS and TDDFT: Results for CIS and TDDFT were reported for a similar test set in Ref. 13. The authors used a basis of triple-ζ quality which is quite close to the basis set limit for these methods. CIS is (as far as energies and relaxed derivatives thereof are concerned) identical to coupled-cluster singles (CCS), which is the first member of the coupled-cluster hierarchy. Therefore, CC2 is expected to be a systematic improvement over CIS. This is confirmed by comparison of the CIS results from Ref. 13 with the present results for CC2. Adiabatic excitation energies at the CIS level often have errors on the order of ± 1.0 eV and the impact of the electronic excitations on the structure is in several cases not correct even at a qualitative level; e.g., nearly no elongation of the carbonyl bond is predicted for aldehydes and for the T_1 state of CH_2S a planar structure is calculated. For molecules with triple bonds, like N_2, CIS sometimes shows a fortuitous error compensation for structures and force constants. However, the energetic separations of the excited states are reproduced only very poorly.

As CC2, TDDFT proves to be a substantial improvement on CIS.[13] Structures and vibrational frequencies in the test set are reproduced relatively well, even for molecules with triple bonds. Compared to CC2, TDDFT has a better tolerance for near-multireference cases and still works well for transition metal compounds and metal clusters. Taking into account the low computational costs, TDDFT certainly is the method of choice for large systems. However, for a given application it often appears difficult to assess the reliability of DFT calculations, since no systematic improvement of the functionals is possible. It may even be difficult to predict the error within a certain class of excitations, as e.g., for the $\pi^* \leftarrow n$ excitation of formaldehyde TDDFT performs well, but it exhibits large errors in excitation energies, structure constants and vibrational frequencies for glyoxal.[13] The most serious problem of TDDFT is its tendency to underestimate excitation energies, partly as a problem of the asymptotic behavior of the standard functionals (some remedies for this problem exist[60]), partly because of the tendency of TDDFT to delocalize electrons, which leads to a pronounced underestimation of excitation energies for charge-transfer states.

The strength of CC2, as compared to TDDFT, is its higher reliability for excitation energies. It is the method of choice for medium sized organic and inorganic main group compounds (up to about 30–50 atoms), as long as they do not have significant multireference character. Its reliability can be assessed by the diagnostics described above and, in addition, for small model molecules the coupled-cluster hierarchy can be applied to test and improve the results.

Downloaded 13 Feb 2004 to 141.52.232.84. Redistribution subject to AIP license or copyright, see http://jcp.aip.org/jcp/copyright.jsp

(h) Comparison with other approximations to CCSD: A number of alternative approximations to CCSD for excited states have been devised within the EOM picture. The first one of these was EOM–CCSD(2)[29] [or EOM–MBPT(2)] which, however, is only interesting for ionization problems, as for excitation energies it still scales with the sixth power of the system size in the iterative steps.[29] Later a partitioned variant, termed P-EOM-MBPT(2), was developed,[9,61] for which only one noniterative $\mathcal{O}(N^6)$-step remains. For geometry optimizations focusing on one particular state, however, this step may still dominate the calculation time, as already noted by the authors of Ref. 9. Only few applications were presented for this method.[9] Most notably, P-EOM-MBPT(2) tends to give too large excitation energies for valence states (both vertical[61] and adiabatic[9]), whereas for excited state structures it may be somewhat superior to CC2. A more interesting alternative to CC2 is constituted by CIS(D) which involves a noniterative $\mathcal{O}(N^5)$-step only. From the data presented in Ref. 8, however, the authors took a rather pessimistic view on the performance of CIS(D) for excited state hypersurfaces. Like CC2 in our study, CIS(D) yields rather erratic results for the structures of CO and N_2. The *trans*-bent state of acetylene is described rather satisfactorily with both CC2 and CIS(D), but for the S_1 state of formaldehyde CC2 seems to be superior to CIS(D). The latter predicts a very small pyramidalization of the carbon atom only. The general problem of CIS(D) is, that it potentially behaves erratically in the case of near degenerate states. This is not the case for CC2, which is closely related to the degenerate extension to CIS(D), CIS(D_∞), devised by Head-Gordon and co-workers.[62]

V. THE $\pi^*\leftarrow\pi$-EXCITED STATE OF *TRANS*-AZOBENZENE

Azobenzene and its derivatives have recently gained considerable interest as building blocks for the development of materials for optical data storage.[63,64] In the previous paper dealing with ground state gradients[34] the CC2 ground state structure of *trans*-azobenzene was reported and compared to the one obtained at the MP2 level. Here, we report the structure of the $\pi^*\leftarrow\pi$ excited state of *trans*-azobenzene, which belongs to the S_2 hypersurface of the system. At this point, we do not want to conceal, that the certainly more interesting S_1 surface constitutes a problem for a single-reference based method as CC2. At a qualitative level, CC2 correctly predicts the molecule to twist around the nitrogen–nitrogen bond. However, this leads directly into the region where the reference determinant changes from $(\pi)^2$ to $(\pi^*)^2$. Of course, CC2 offers no reliable description of this situation and therefore it is not possible to establish whether only one minimum exists along the reaction path leading to the *cis*-isomer.

The $\pi^*\leftarrow\pi$ excited state is less problematic, we find a planar structure which was confirmed by a vibrational normal mode analysis (*vide infra*). The structure constants obtained with different basis sets are displayed in Table VIII (compare also Fig. 3). Basis set effects are moderate: changing from cc-pVDZ to cc-pVTZ, the adiabatic excitation energy is lowered by 0.1 eV and bonds shorten by typically 1 pm. Additional diffuse functions have only some moderate effect on the excitation energy and the structure parameters change by less than 0.2 pm only.

With respect to the CC2 ground state structure, the elongation of the azo-bond is the most obvious structural change. It is accompanied by a shortening of the nitrogen–carbon bond and a quinoidal distortion of the phenyl moieties. This reflects the charge-transfer character of this state: electron density is transferred from the central azo group towards the aromatic rings. The lengthening of the N═N bond is probably too pronounced in the CC2 model, as perturbation theory will be biased by a low-lying $(\pi^*)^2$ state as the bond is stretched. The D_1 diagnostic is low (0.03), but the D_2 diagnostic (0.24) indeed indicates a low-lying doubly excited state, which is also reflected in a rather high double-excitation contribution of 11.6%.

The minimum character of the planar structure was assessed by calculating the harmonic force field. To save computation time, this was only done at the double-ζ level, which is expected to yield a qualitatively correct result. Another calculation of the harmonic force field was carried out for the ground state. The calculations confirm the planar structures for both ground and excited state. We do not want to discuss the vibrational spectra in detail, since this is beyond the scope of the present communication.

The difference in the zero-point vibrational energy between ground and excited state can be used together with the aug-cc-pVTZ result for T_e to estimate the 0–0 transition as 3.5 eV. In the experimental gas-phase spectrum the lowest vibrational band can be assumed in the region between 3.65 and 3.75 eV,[65] which correlates rather well with the CC2 result.

The current result is in agreement with a theoretical study by Ishikawa *et al.*[66] who calculated two minima on the S_2 hypersurface corresponding to a *trans*- and *cis*-isomer, respectively. This finding revised the potential curves by Monti *et al.*,[67] who concluded that the $\pi^*\leftarrow\pi$ excitation would lead to a photoisomerization along the rotation pathway. A planar S_2 state is also consistent with recent femtosecond spectroscopic experiments,[68] which indicate that no photoisomerization takes place after $\pi^*\leftarrow\pi$ excitation, but that internal conversion to S_1 is the nearly exclusive decay path.

VI. CONCLUSIONS

We have presented an implementation of excited state gradients for the coupled-cluster model CC2, which employs the resolution-of-the-identity approximation. The expressions obtained can be cast into a formulation that resembles much the one for the ground state gradient. Similar as the underlying implementation of RI–CC2 excitation energies,[32] the code features a low resource consumption with main memory requirements scaling as $\mathcal{O}(N^2)$ and mass storage scaling as $\mathcal{O}(N^3)$. Of course, the asymptotic scaling of the computation time is still $\mathcal{O}(N^5)$, as demonstrated by numerical examples. Developments towards lower scaling coupled-cluster methods using the local ansatz have been recently

Downloaded 13 Feb 2004 to 141.52.232.84. Redistribution subject to AIP license or copyright, see http://jcp.aip.org/jcp/copyright.jsp

TABLE VIII. Calculated structure parameters of the $^1B_u(\pi^*\leftarrow\pi)$ state of *trans*-azobenzene (C_{2h}), using RI–CC2 and different basis sets (the corresponding auxiliary basis sets from Ref. 39 were used).

	cc-pVDZ	cc-pVTZ		aug-cc-pVTZ
T_e	3.728	3.616		3.538
ν_{0-0}	3.675			(expt.[a]: 3.65–3.75)
		Bond lengths (pm)		
N═N	139.34	139.00	(+11.47)[b]	139.09
N–C1	136.66	135.88	(−5.99)	135.91
C_1-C_2	144.21	143.04	(+3.24)	143.06
C_1-C_6	144.81	143.71	(+3.48)	143.74
C_2-C_3	139.07	137.81	(−1.54)	137.83
C_6-C_5	139.59	138.41	(−0.57)	138.48
C_3-C_4	142.25	141.12	(+1.63)	141.20
C_4-C_5	141.61	140.36	(+0.36)	140.39
C_2-H	109.59	108.27	(+0.06)	108.36
C_6-H	109.31	108.00	(−0.17)	108.12
C_3-H	109.57	108.22	(+0.15)	108.30
C_5-H	109.64	108.28	(+0.06)	108.36
C_4-H	109.62	108.27	(+0.07)	108.34
		Bond angles (deg)		
C_1-N-N	109.57	109.73	(−3.90)	109.82
C_2-C_1-N	116.49	116.55	(+1.46)	116.42
C_6-C_1-N	125.11	124.90	(+0.31)	124.86
$C_2-C_1-C_6$	118.41	118.55	(−1.77)	118.71
$C_1-C_2-C_3$	120.77	120.64	(+0.59)	120.54
$C_1-C_6-C_5$	119.81	119.72	(+0.43)	119.61
$C_2-C_3-C_4$	120.14	120.18	(+0.39)	120.18
$C_6-C_5-C_4$	120.88	120.85	(+0.34)	120.84
$C_3-C_4-C_5$	119.99	120.06	(+0.03)	120.12
$H-C_2-C_1$	117.10	117.37	(−0.92)	117.42
$H-C_6-C_1$	117.23	117.53	(−1.48)	117.68
$H-C_3-C_2$	120.11	120.11	(+0.08)	120.16
$H-C_5-C_6$	119.71	119.73	(+0.02)	119.75
$H-C_4-C_3$	119.94	119.89	(−0.16)	119.85

[a]Experimental value estimated from spectrum in Ref. 65.

[b]Values in parentheses are the difference to the CC2/cc-pVTZ ground state geometry (Ref. 34) ($R_e^{\pi\pi^*}-R_e^0$).

reported,[69,70] but these methods are still at their early stages and encounter relatively large errors in the excitation energies.

The efficiency and stability of the current implementation is demonstrated by several applications including polyene chains with up to 62 atoms (1348 basis functions). For medium-sized molecules and for calculations with diffuse basis sets, the analysis of the computation times reveals a bottleneck due to contributions from the SCF part, which is still carried out with conventional four-index integrals. As a possible remedy we suggest a combination of RI–CC2 with the recently published RI-SCF approach.[48]

In order to assess the accuracy of CC2, adiabatic excitation energies, excited state structures, and vibrational frequencies of 20 small molecules were examined. We find that especially for excitation energies CC2 gives very promising results. Except for cases with strong multireference character, which can be identified on grounds of the diagnostic values discussed in Sec. IV, the average error for valence excitations is in the order of ± 0.3 eV. A problem is reported

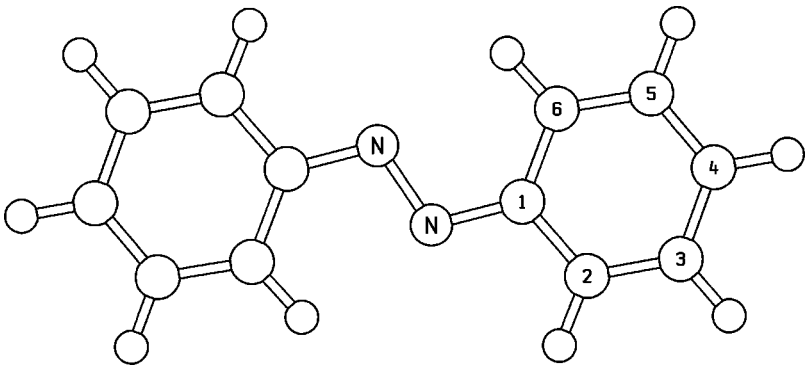


FIG. 3. Numbering of atoms in *trans*-azobenzene for Table VIII.

Downloaded 13 Feb 2004 to 141.52.232.84. Redistribution subject to AIP license or copyright, see http://jcp.aip.org/jcp/copyright.jsp

for the Rydberg excitation of water, which is too low by 0.8 eV.

As for the ground state, CC2 tends to give too long bond distances, especially if multiple bonds are involved. The corresponding vibrational normal modes consequently have somewhat too low frequencies. With exception of the cumulene C_3, however, predicted structural changes are in all considered cases qualitatively correct. Of course, due to the single reference character of the underlying ground state method, bond breaking problems like the isomerization of azobenzene along the rotation pathway are out of reach for CC2.

Comparing to results from a previous study focusing on TDDFT, RPA, and CIS,[13] it can be concluded that CC2 improves systematically over CIS. Similarly, the findings of Ref. 13 suggest TDDFT as a general replacement of CIS for large-scale calculations. As compared to CC2, TDDFT has a somewhat larger tolerance for multireference cases and therefore a broader range of applicability. However, it is not in all cases reliable and unfortunately lacks a possibility for systematic improvements. Thus, RI–CC2 is a useful alternative to TDDFT for medium-sized systems with single-reference character.

ACKNOWLEDGMENT

This work was supported by the Center for Functional Nanostructures (CFN) of the Deutsche Forschungsgemeinschaft (DFG) within project C2.1.

[1] P. Pulay, Mol. Phys. **17**, 197 (1969).
[2] P. Pulay, Mol. Phys. **18**, 473 (1970).
[3] Y. Osamura, Y. Yamaguchi, and H. F. Schaefer III, J. Chem. Phys. **77**, 383 (1982).
[4] N. Yamamoto, T. Vreven, M. A. Robb, M. J. Frisch, and H. B. Schlegel, Chem. Phys. Lett. **250**, 373 (1996).
[5] J. B. Foresman, M. Head-Gordon, J. A. Pople, and M. J. Frisch, J. Phys. Chem. **96**, 135 (1992).
[6] J. Cioslowski and J. V. Ortiz, J. Chem. Phys. **96**, 8379 (1992).
[7] J. F. Stanton and J. Gauss, J. Chem. Phys. **100**, 4695 (1994).
[8] J. F. Stanton, J. Gauss, N. Ishikawa, and M. Head-Gordon, J. Chem. Phys. **103**, 4160 (1995).
[9] B. R. J. Gwaltney, J. Chem. Phys. **110**, 62 (1999).
[10] R. Shepard, H. Lischka, P. G. Szalay, T. Kovar, and M. Ernzerhof, J. Chem. Phys. **96**, 2085 (1992).
[11] H. Lischka and M. Dallos, Mol. Phys. **100**, 1647 (2002).
[12] C. van Caillie and R. Amos, Chem. Phys. Lett. **308**, 249 (1999).
[13] F. Furche and R. Ahlrichs, J. Chem. Phys. **117**, 7433 (2002).
[14] A. Bernhardsson, N. Forsberg, P.-Å. Malmqvist, B. O. Roos, and L. Serrano-Andrès, J. Chem. Phys. **112**, 2798 (2000).
[15] Y. Bomble, K. Sattelmeyer, J. Stanton, and J. Gauss (unpublished).
[16] O. Christiansen, H. Koch, and P. Jørgensen, Chem. Phys. Lett. **243**, 409 (1995).
[17] J. L. Whitten, J. Chem. Phys. **58**, 4496 (1973).
[18] B. I. Dunlap, J. W. D. Conolly, and J. R. Sabin, J. Chem. Phys. **71**, 3396 (1979).
[19] O. Vahtras, J. E. Almlöf, and M. W. Feyereisen, Chem. Phys. Lett. **213**, 514 (1993).
[20] R. J. Bartlett, in *Modern Electronic Structure Theory*, edited by D. R. Yarkony (World Scientific, Singapore, 1995), Vol. 2, pp. 1047.
[21] T. Helgaker, P. Jørgensen, and J. Olsen, *Molecular Electronic-Structure Theory* (Wiley, New York, 2000).
[22] H. J. Monkhorst, Int. J. Quantum Chem. **S11**, 421 (1977).
[23] J. Stanton and R. Bartlett, J. Chem. Phys. **98**, 7029 (1993).
[24] H. Koch and P. Jørgensen, J. Chem. Phys. **93**, 3333 (1990).
[25] H. Koch, H. J. A. Jensen, P. Jørgensen, and T. Helgaker, J. Chem. Phys. **93**, 3345 (1990).
[26] J. F. Stanton, J. Chem. Phys. **99**, 8840 (1993).
[27] J. F. Stanton and J. Gauss, Theor. Chim. Acta **91**, 267 (1995).
[28] O. Christiansen, J. F. Stanton, and J. Gauss, J. Chem. Phys. **108**, 3987 (1997).
[29] J. F. Stanton and J. Gauss, J. Chem. Phys. **103**, 1064 (1995).
[30] M. Head-Gordon, R. J. Rico, M. Oumi, and T. J. Lee, Chem. Phys. Lett. **219**, 21 (1994).
[31] O. Christiansen, J. Gauss, J. F. Stanton, and P. Jørgensen, J. Chem. Phys. **111**, 525 (1999).
[32] C. Hättig and F. Weigend, J. Chem. Phys. **113**, 5154 (2000).
[33] C. Hättig and A. Köhn, J. Chem. Phys. **117**, 6939 (2002).
[34] C. Hättig, J. Chem. Phys. **118**, 7751 (2003).
[35] O. Christiansen, P. Jørgensen, and C. Hättig, Int. J. Quantum Chem. **68**, 1 (1998).
[36] P. Szalay, Int. J. Quantum Chem. **55**, 151 (1995).
[37] H. Koch, O. Christiansen, R. Kobayashi, P. Jørgensen, and T. Helgaker, Chem. Phys. Lett. **228**, 233 (1994).
[38] T. Helgaker and P. Jørgensen, Adv. Quantum Chem. **19**, 183 (1988).
[39] F. Weigend, A. Köhn, and C. Hättig, J. Chem. Phys. **116**, 3175 (2002).
[40] See EPAPS Document No. E-JCPSA6-119-304334 for additional tables (one- and two-particle densities, RI-intermediates, and auxiliary basis sets for lithium and magnesium). A direct link to this document may be found in the online article's HTML reference section. The document may also be reached via the EPAPS homepage (http://www.aip.org/pubservs/epaps.html) or from ftp.aip.org in the directory /epaps/. See the EPAPS homepage for more information.
[41] N. C. Handy and H. F. Schaefer, J. Chem. Phys. **81**, 5031 (1984).
[42] J. F. Stanton and J. Gauss, J. Chem. Phys. **101**, 3001 (1994).
[43] K. Hald, D. Yeager, C. Hättig, and P. Jørgensen, Chem. Phys. Lett. **328**, 291 (2000).
[44] K. Hald, C. Hättig, and P. Jørgensen, J. Chem. Phys. **113**, 7765 (2000).
[45] K. Hald, C. Hättig and P. Jørgensen, J. Chem. Phys. **115**, 3545 (2001).
[46] C. Hättig, A. Köhn, and K. Hald, J. Chem. Phys. **116**, 5401 (2002).
[47] C. Hättig and K. Hald, Phys. Chem. Chem. Phys. **4**, 2111 (2002).
[48] F. Weigend, Phys. Chem. Chem. Phys. **4**, 4285 (2002).
[49] F. Weigend and M. Häser, Theor. Chem. Acc. **97**, 331 (1997).
[50] F. Weigend, M. Häser, H. Patzelt, and R. Ahlrichs, Chem. Phys. Lett. **294**, 143 (1998).
[51] J. F. Stanton, J. Gauss, W. J. Lauderdale, J. D. Watts, and R. J. Bartlett. ACESII an *ab initio* program system, 2002. The package also contains modified versions of the MOLECULE Gaussian integral program of J. Almlöf and P. R. Taylor, the ABACUS integral derivative program written by T. Helgaker, H. J. Aa. Jensen, P. Jørgensen, and P. R. Taylor, and the PROPS property evaluation integral code of P. R. Taylor.
[52] K. W. Sattelmeyer, J. F. Stanton, J. Olsen, and J. Gauss, Chem. Phys. Lett. **347**, 499 (2001).
[53] T. H. Dunning, J. Chem. Phys. **90**, 1007 (1989).
[54] D. E. Woon and T. H. Dunning, J. Chem. Phys. **100**, 2975 (1994).
[55] C. L. Janssen and I. M. B. Nielsen, Chem. Phys. Lett. **290**, 423 (1998).
[56] I. M. B. Nielsen and C. L. Janssen, Chem. Phys. Lett. **310**, 568 (1999).
[57] O. Christiansen, H. Koch, P. Jørgensen, and J. Olsen, Chem. Phys. Lett. **256**, 185 (1996).
[58] O. Christiansen and P. Jørgensen, J. Am. Chem. Soc. **120**, 3423 (1998).
[59] K. L. Bak, J. Gauss, P. Jørgensen, J. Olsen, T. Helgaker, and J. F. Stanton, J. Chem. Phys. **114**, 6548 (2001).
[60] M. E. Casida, C. Jamorski, K. C. Casida, and D. R. Salahub, J. Chem. Phys. **108**, 4439 (1998).
[61] S. R. Gwaltney, M. Nooijen, and R. J. Bartlett, Chem. Phys. Lett. **248**, 189 (1996).
[62] M. Head-Gordon, M. Oumi, and D. Maurice, Mol. Phys. **96**, 593 (1999).
[63] R. Hagen and T. Bieringer, Adv. Mater. (Weinheim, Ger.) **13**, 1805 (2001).
[64] P. H. Rasmussen, P. S. Ramanujan, S. Hvilsted, and R. H. Berg, J. Am. Chem. Soc. **121**, 4738 (1999).
[65] J.-Å. Andersson, R. Petterson, and L. Tegnèr, J. Photochem. **20**, 17 (1982).
[66] T. Ishikawa, T. Noro, and T. Shoda, J. Chem. Phys. **115**, 7503 (2001).
[67] S. Monti, G. Orlandi, and P. Palmeri, Chem. Phys. **71**, 87 (1982).
[68] T. Fujino, S. Y. Arzhantsev, and T. Tahara, Bull. Chem. Soc. Jpn. **75**, 1031 (2002).
[69] T. Korona and H.-J. Werner, J. Chem. Phys. **118**, 3006 (2003).
[70] T. D. Crawford and R. A. King, Chem. Phys. Lett. **366**, 611 (2002).

Downloaded 13 Feb 2004 to 141.52.232.84. Redistribution subject to AIP license or copyright, see http://jcp.aip.org/jcp/copyright.jsp

[71] K. P. Huber and G. Herzberg, *Molecular Spectra and Molecular Structure: IV. Constants of Diatomic Molecules* (Van Nostrand Reinhold, New York, 1979).
[72] D. J. Clouthier and J. Karolczak, J. Chem. Phys. **94**, 1 (1991).
[73] D. J. Clouthier and D. A. Ramsay, Annu. Rev. Phys. Chem. **34**, 31 (1983).
[74] K. P. Huber and G. Herzberg, *Molecular Spectra and Molecular Structure: III. Electronic Spectra and Electronic Structure of Polyatomic Molecules* (Van Nostrand Reinhold, New York, 1966).
[75] T. R. Huet, M. Godefroid, and M. Herman, J. Mol. Spectrosc. **114**, 32 (1990).
[76] J. M. Hollas, ''Molecular structure from rotational and vibrational transitions in electronic spectra,'' in *Recent Experimental and Computational Advances in Molecular Spectroscopy*, edited by R. Fausto (Kluwer, Dordrecht, 1993), pp. 27–61.
[77] R. Y. Dong, R. Nanes, and D. A. Ramsay, Can. J. Chem. **71**, 1595 (1993).
[78] J. C. D. Brand, J. H. Calloman, and J. K. G. Watson, Discuss. Faraday Soc. **35**, 175 (1963).
[79] M. Drabbels, W. L. Meerts, and J. J. ter Meulen, J. Chem. Phys. **99**, 2352 (1993).
[80] The conventions $\tau_{pq}=1/2\Sigma_\sigma a^\dagger_{p\sigma}a_{q\sigma}$ (where $a^\dagger$ and a are creation and annihilation operators, respectively, and Σ_σ indicates spin summation), $\tau_{pqrs}=\tau_{pq}\tau_{rs}$ and $\tau^{(-)}_{pqrs}=\tau_{pq}\tau_{rs}-\delta_{qr}\tau_{ps}$ are used. The usual symbols E_{pq} (and e_{pqrs}) may be confused with the notation for the excitation vectors $\bar{E}^f$, E^f.

Downloaded 13 Feb 2004 to 141.52.232.84. Redistribution subject to AIP license or copyright, see http://jcp.aip.org/jcp/copyright.jsp